

ORIGINAL RESEARCH ARTICLE

Coiled-coil domain-containing protein 51 as an independent prognostic marker in hepatocellular carcinoma: Implications for tumor progression and immune infiltration

Siqi Huang¹, Zhang Chen¹, Wei Yu¹, and Xiaoyan Huang^{*1}

Department of Ultrasound, The Second Affiliated Hospital and Yuying Children's Hospital of Wenzhou Medical University, Wenzhou, Zhejiang, China

Abstract

Hepatocellular carcinoma (HCC) is a leading cause of cancer-related mortality worldwide. Although the coiled-coil domain-containing protein 51 (CCDC51) has been implicated in retinal pathologies, its function in HCC remains poorly defined. Here, we report that reduced CCDC51 expression is associated with favorable clinical outcomes in HCC patients. Bioinformatic analyses revealed significant correlations between CCDC51 levels and multiple tumor characteristics, including immune cell infiltration, the tumor microenvironment, and microsatellite instability status. Notably, multivariate Cox regression and nomogram analyses established CCDC51 as an independent prognostic biomarker for HCC. Pathway enrichment studies further linked elevated CCDC51 expression to dysregulation of RNA transport and Wnt signaling. Functionally, genetic silencing of *CCDC51* in HCC cell lines resulted in significant suppression of proliferation, migration, and invasion. Collectively, these findings identify CCDC51 as a novel prognostic marker and a potential therapeutic target in HCC.

Keywords: Coiled-coil domain-containing protein 51; Biomarker; Hepatocellular carcinoma; Immune cell infiltration; Proliferation

***Corresponding author:**
Xiaoyan Huang
(221180@wzhealth.com)

Citation: Huang S, Chen Z, Yu W, Huang X. Coiled-coil domain-containing protein 51 as an independent prognostic marker in hepatocellular carcinoma: Implications for tumor progression and immune infiltration. *Cancer Plus*. 2026;8(1):025480084. doi: 10.36922/CP025480084

Received: November 27, 2025

Revised: January 7, 2026

Accepted: January 12, 2026

Published online: February 10, 2026

Copyright: © 2026 Author(s). This is an Open-Access article distributed under the terms of the Creative Commons Attribution License, permitting distribution, and reproduction in any medium, provided the original work is properly cited.

Publisher's Note: AccScience Publishing remains neutral with regard to jurisdictional claims in published maps and institutional affiliations.

1. Introduction

Hepatocellular carcinoma (HCC) is the fourth most common cause of cancer-related death worldwide and represents the second most frequently diagnosed malignancy in China.^{1,2} HCC development is strongly associated with underlying risk factors, such as chronic hepatitis B virus or hepatitis C virus infection, cirrhosis, non-alcoholic fatty liver disease, and metabolic disorders, although the precise molecular mechanisms remain incompletely elucidated.³ Due to frequent late-stage diagnosis, a significant proportion of patients are not eligible for curative interventions, such as surgical resection or liver transplantation. Current non-surgical treatments, including chemotherapy—either as monotherapy or combined with radiotherapy—often yield suboptimal outcomes, contributing to high mortality rates among advanced HCC patients.⁴ There is a critical need to identify specific biomarkers correlated with hepatocarcinogenesis to facilitate early detection and guide personalized therapeutic strategies.

The rapid advances in digital systems and diverse databases have enabled the widespread adoption of bioinformatics approaches in oncology studies.^{5,6} Coiled-coil domain-containing protein 51 (CCDC51), a protein characterized by coiled-coil domains, has been associated with retinal conditions.⁷ This evolutionarily conserved protein harbors a central coiled-coil domain that supports protein–protein interactions and subcellular scaffolding mechanisms. However, the role of CCDC51 in the diagnostic and prognostic evaluation of HCC, as well as its contribution to immune modulation, remains inadequately explored.

This investigation assessed the expression profiles and clinical prognostic significance of *CCDC51* across diverse human malignancies. Cell-based functional analyses indicated that *CCDC51* is a potential therapeutic target for HCC and may function as a biomarker for its diagnosis and prognostic assessment.

2. Materials and methods

2.1. Analyses of *CCDC51* in human cancer

Publicly available data from The Cancer Genome Atlas (TCGA) (<https://www.cancer.gov/about-nci/organization/ccg/research/structural-genomics/tcga>) and the genotype-tissue expression (GTEx) portal were employed to analyze *CCDC51* expression patterns across multiple cancer types. To assess the pan-cancer protein expression profile of CCDC51, we analyzed data from the Clinical Proteomic Tumor Analysis Consortium. This comprehensive proteomic dataset provides quantitative protein expression levels across multiple human malignancies. The gene expression profiling interactive analysis (GEPIA)⁸ and PrognScan databases⁹ were utilized to assess the prognostic significance of *CCDC51* in multiple cancer types.

2.2. Receiver operating characteristic (ROC) curve analysis

To evaluate the diagnostic value of the identified signature genes, the pROC package in R software (v4.0.3, R Foundation for Statistical Computing, Austria) was utilized to construct ROC curves and determine the corresponding area under the curve (AUC) values.

2.3. Single-cell sequencing and spatial transcriptome analyses

The single-cell sequencing data and spatial transcriptome analysis were processed using the Sparkle web platform (<https://www.grswsci.top/analyze/>).^{10,11}

2.4. Tumor mutation burden (TMB) and microsatellite instability (MSI) analyses

TMB is derived by Thorsson *et al.*¹² MSI is derived by Bonneville *et al.*¹³ Statistical analysis was conducted using R software. Results were considered statistically significant at $p < 0.05$.

2.5. Immune infiltration analysis

The tumor immune estimation resource (TIMER) platform (<https://cistrome.shinyapps.io/timer/>) was utilized to quantify immune infiltration levels and investigate the immune-related functions of *CCDC51*.¹⁴ To accurately assess immune correlation, we used the TIMER and xCell algorithms in the immunedeconv R software package.

2.6. Cell culture, siRNA, and quantitative reverse transcription polymerase chain reaction

The HCCLM3 and Hep3B cell lines were acquired from the American Type Culture Collection (ATCC) (ATCC, USA) and maintained in RPMI-1640 medium containing 10% fetal bovine serum (FBS) (Biological Industries USA, Inc., USA). *CCDC51* siRNA kits were used in this study (Gene Pharma, China), with sequences as follows: si-CCDC51#1: 5'-GUGCUCUACAUGCUAUUCAAAGCCA-3' and si-CCDC51#2: 5'-AUUCAUGUCUAGAAGGC UUACGAGA-3'. Following the manufacturer's instructions, transfection was performed using Lipofectamine 3000 (Invitrogen, USA).

Quantitative reverse transcription polymerase chain reaction was performed according to the manufacturer's standardized procedures. For normalization purposes, β -actin expression served as the endogenous reference. This investigation employed the following oligonucleotide primer sets: For *CCDC51* amplification, forward primer: 5'-GCCTGTGCTCTACATGCTATTC-3' and reverse primer: 5'-CTCGCTTCATTGCTACGATTCT-3' were utilized; regarding β -actin detection, the forward primer sequence was 5'-CACTCTTCCAGCCTTCCTTC-3', while the reverse primer was 5'-GTACAGGTCTTTGCGGA TGT-3'.

2.7. Western blot

Protein extraction was performed using radioimmunoprecipitation assay lysis buffer, followed by separation using sodium dodecyl sulfate–polyacrylamide gel electrophoresis. For immunoblot analysis, the electrophoresed proteins were transferred onto polyvinylidene fluoride membranes. To minimize nonspecific interactions, these membranes were blocked with 10% nonfat milk solution for 2 h at room temperature.

The membranes were then incubated with primary antibodies, including anti-CCDC51 (ab121329, Abcam, UK) and anti- β -actin (ab8226, Abcam, UK), followed by exposure to appropriate horseradish peroxidase-conjugated secondary antibodies (RGAM001 and RGAR001, Proteintech, UK). Protein bands were visualized using an enhanced chemiluminescence detection system (SuperSignal™ West Pico PLUS Chemiluminescent Substrate, Pierce, USA) for signal development.

2.8. Cell counting kit-8 assay

Cells were seeded in 96-well plates at a density of 2×10^3 cells per well. According to the manufacturer's protocol, cellular proliferation was evaluated using a Cell Counting Kit-8 (40203ES60, Yeasen, China).

2.9. Transwell migration and invasion assays

For invasion assays, transwell inserts were initially coated with matrigel (BD Biosciences, USA). A suspension of 4×10^4 cells in 100 μ L of serum-free medium was introduced into each upper compartment. Concurrently, the lower compartment received 600 μ L of medium supplemented with 20% FBS. Following incubation, non-invading cells on the upper membrane surface were removed by FBS washing and fixed using paraformaldehyde. Migrated cells on the lower side were stained with crystal violet and visualized under an inverted microscope (Leica DMi1, Leica Microsystems, USA).

2.10. Immunohistochemical validation

Immunohistochemistry data from the Human Protein Atlas (HPA, <https://www.proteinatlas.org/>) were utilized to evaluate CCDC51 protein levels in both HCC and corresponding normal tissues.

2.11. Statistical analysis

The statistical relevance of the differences observed among groups was assessed using Student's *t*-test, and $p < 0.05$ was considered statistically significant.

3. Results

3.1. The expression and prognosis values of CCDC51 in human cancers

To assess CCDC51 expression across multiple malignancies, we first analyzed TCGA data. CCDC51 showed elevated expression in 16 cancer types relative to matched normal samples. In contrast, decreased CCDC51 levels were observed in three other cancer types (Figure 1A).

Integration of datasets from GTEx and TCGA demonstrated markedly elevated CCDC51 transcript levels in 24 cancer types (Figure 1B). To evaluate CCDC51

protein expression in human cancers, we analyzed clinical proteomic tumor analysis consortium data and identified high expression in four distinct malignancies. Conversely, reduced protein levels were detected in three other cancer types (Figure 1C). Collectively, these results indicate CCDC51 may contribute to regulatory mechanisms in diverse tumors.

To further investigate the clinical relevance of CCDC51 expression, we assessed its prognostic potential across multiple cancers. Elevated CCDC51 levels were associated with poorer overall survival (OS) in eight malignancies (Figure 1D). These findings indicate that CCDC51 may serve as a prognostic biomarker across diverse cancer types.

3.2. CCDC51 as a potential cancer biomarker

Ongoing investigations focused on evaluating CCDC51 as a pan-cancer biomarker. Assessment of ROC curves demonstrated that CCDC51 exhibited high diagnostic sensitivity and specificity (AUC > 0.75) across 24 distinct cancer types (Figure 2A-F).

3.3. Gene mutation landscape of CCDC51 in human cancers

Mutational data for CCDC51 were obtained from the cBioPortal database.¹⁴ Mutation frequencies in mature B-cell neoplasms, kidney renal clear cell carcinoma, endometrial carcinoma, and melanoma exceeded those in other cancers (Figure 3A), with gene amplification representing the most frequent alteration type (Figure 3B). A total of 51 missense and 7 truncation mutations were identified within the 0–411 amino acid region of CCDC51 (Figure 3C). Furthermore, copy number variations of CCDC51 were found to modulate its expression, either increasing or decreasing transcript levels across various malignancies (Figure 3D and E).

3.4. DNA methylation of CCDC51 in human cancers

DNA methylation is a key epigenetic mechanism in cancer progression.^{15,16} We therefore examined whether CCDC51 expression is modulated by DNA methylation and assessed its dysregulation across malignancies. An inverse correlation between CCDC51 expression and DNA methylation levels was observed across 13 cancer types (Figure 4A). We further employed TCGA data to evaluate associations between DNA methylation and CCDC51 expression, which demonstrated significant relationships in several cancers (Figure 4B).

3.5. TMB and MSI analysis of CCDC51 in human cancers

TMB is established as a predictive biomarker for immune checkpoint blockade (ICB) therapy.^{17–19} We next assessed the

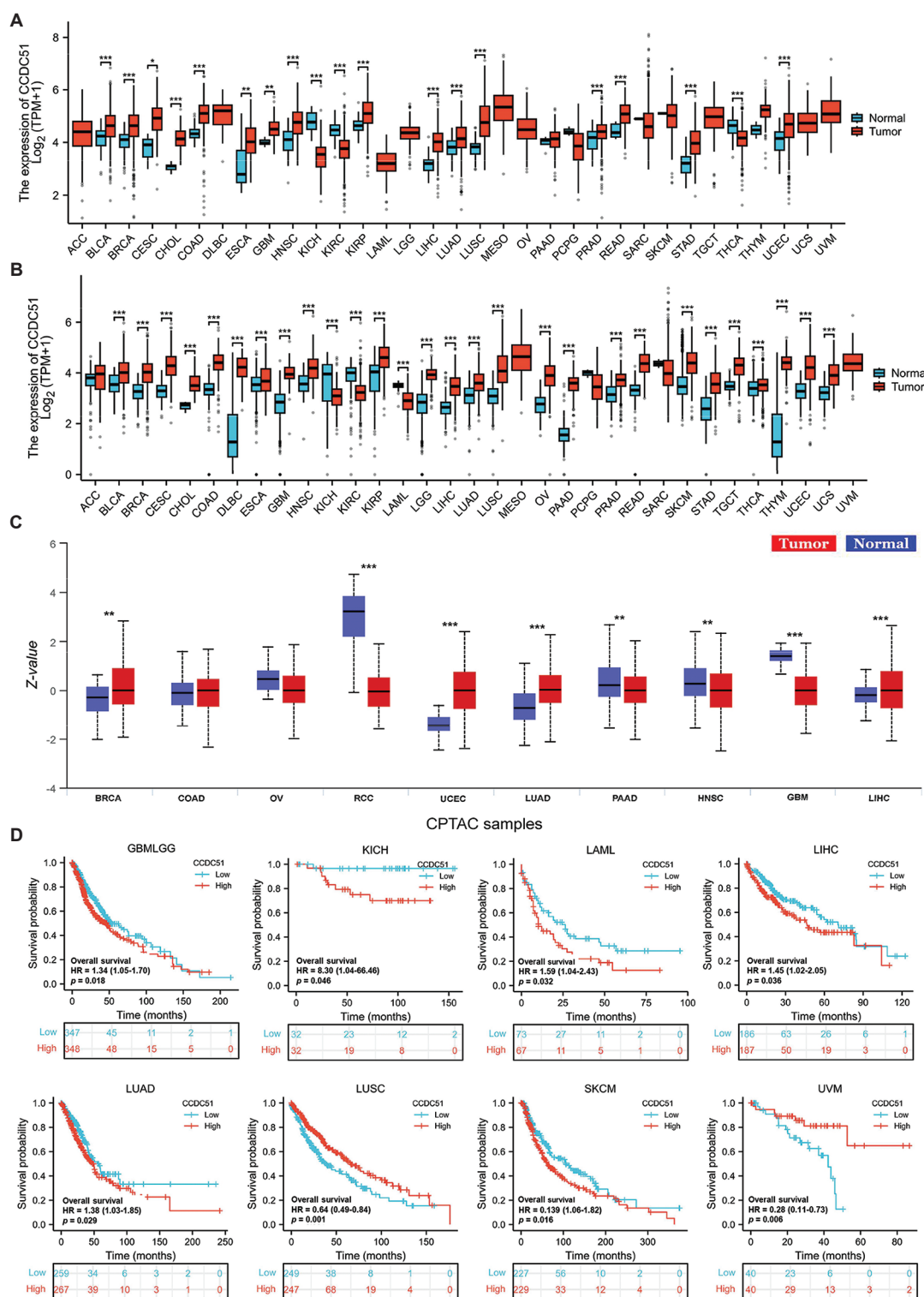


Figure 1. *CCDC51* expression profiles and prognostic implications in human malignancies. (A) Analysis of *CCDC51* expression across various cancers via the TIMER database. (B) Pan-cancer *CCDC51* expression patterns obtained from TCGA and GTEx datasets. (C) Comprehensive analysis of *CCDC51* protein abundance in various malignancies via the CPTAC resource. (D) Overall survival of TCGA cancer patients expressing *CCDC51*.

Notes: * $p < 0.05$; ** $p < 0.01$; *** $p < 0.001$.

Abbreviations: *CCDC51*: Coiled-coil domain-containing protein 51; CPTAC: Clinical proteomic tumor analysis consortium; GTEx: Genotype-tissue expression; HR: Hazard ratio; TCGA: The Cancer Genome Atlas; TIMER: Tumor immune estimation resource; TPM: Transcript per million.

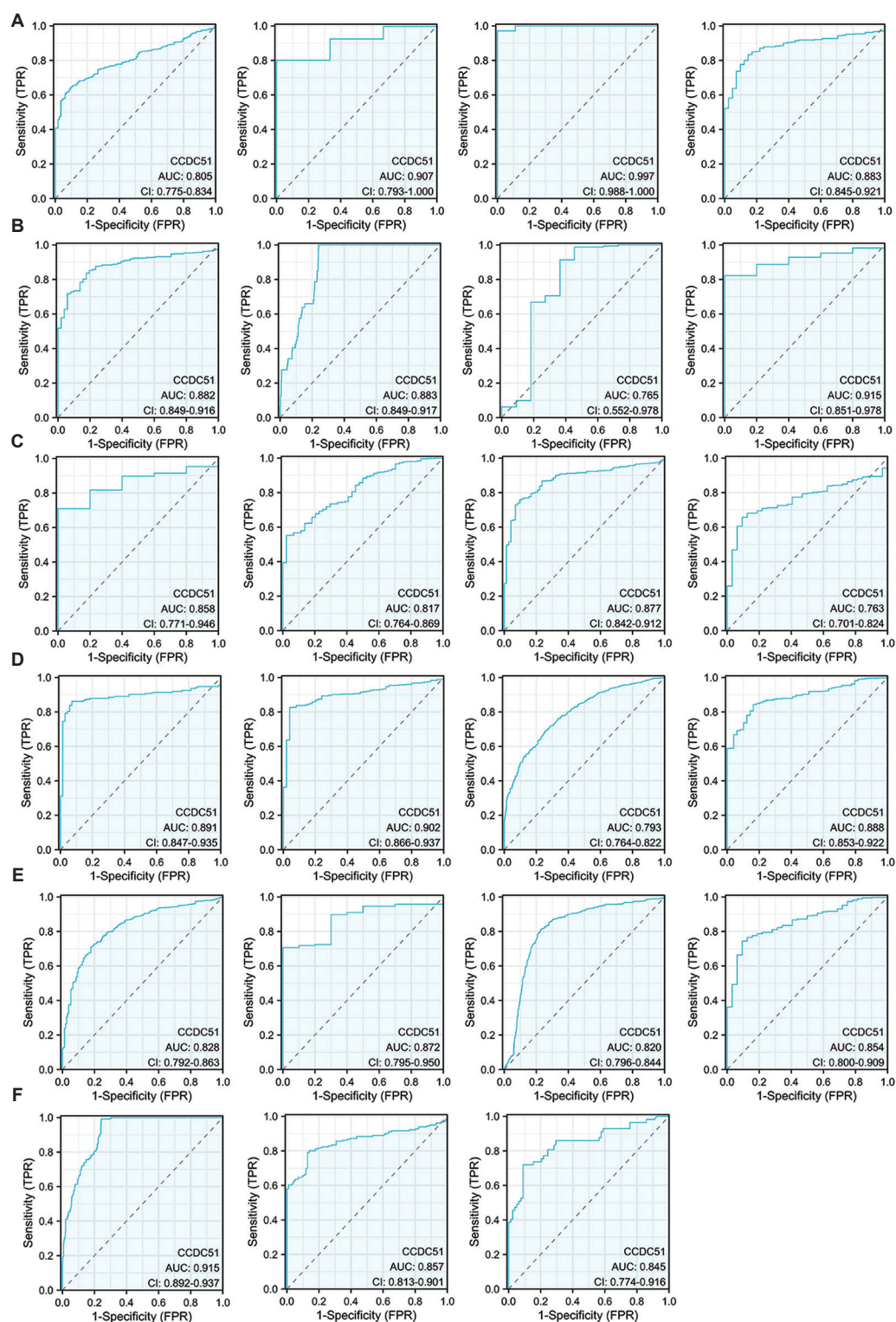


Figure 2. Receiver operating curve analysis evaluating the prognostic predictive value of CCDC51 expression. (A) BRCA, CESC, CHOL, and COAD; (B) COADREAD, DLBC, ESCA, and GBM; (C) GBMLGG, HNSC, KIRC, and KIRP; (D) LAML, LIHC, LUAD, and LUSC; (E) PRAD, READ, SKCM, and STAD; and (F) THYM, UCEC, and UCS.

Abbreviations: AUC: Area under the curve; CCDC51: Coiled-coil domain-containing protein 51; CI: Confidence interval; FPR: False positive rate; TPR: True positive rate.

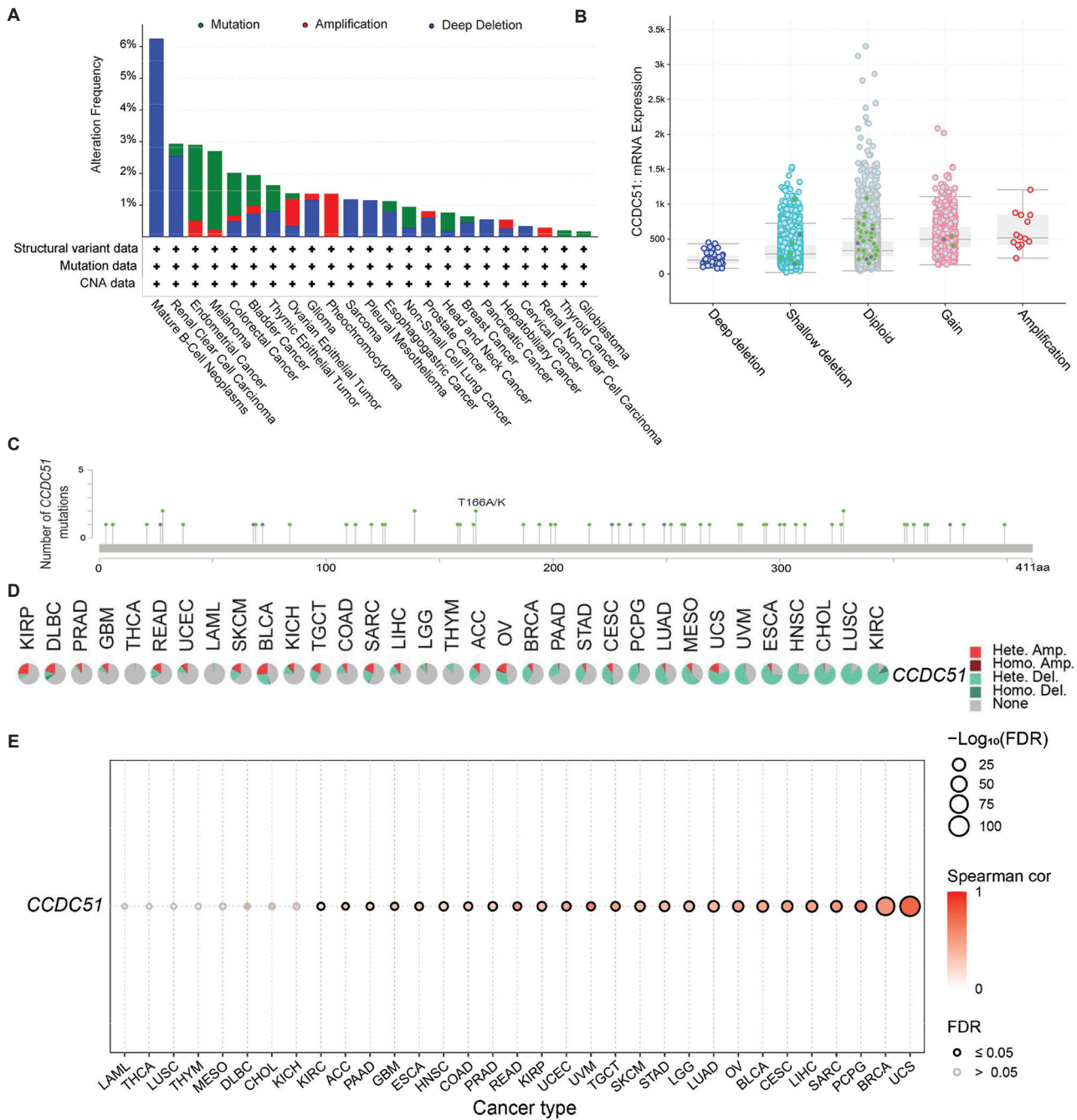


Figure 3. Mutational analysis of *CCDC51*. (A) Distribution of various mutation types in *CCDC51* across multiple cancer types. (B) Mutation frequency of *CCDC51* assessed using the cBioPortal database. (C) Identification of mutational hotspots within the *CCDC51* gene. (D) Percentage of *CCDC51* CNV in each cancer type. (E) Correlation between *CCDC51* CNV and mRNA expression levels across cancers. Abbreviations: CNA: Copy number alteration; CNV: Copy number variation; FDR: False discovery rate.

relationship between *CCDC51* expression and TMB across various malignancies. A positive correlation was observed across 21 cancer types, while an inverse relationship was found in 7 other malignancies (Figure 5A).

Deficient DNA repair mechanisms contribute to hypervariability in DNA sequences.²⁰ We also evaluated correlations between *CCDC51* expression and MSI in multiple cancers. Positive associations were found in 17

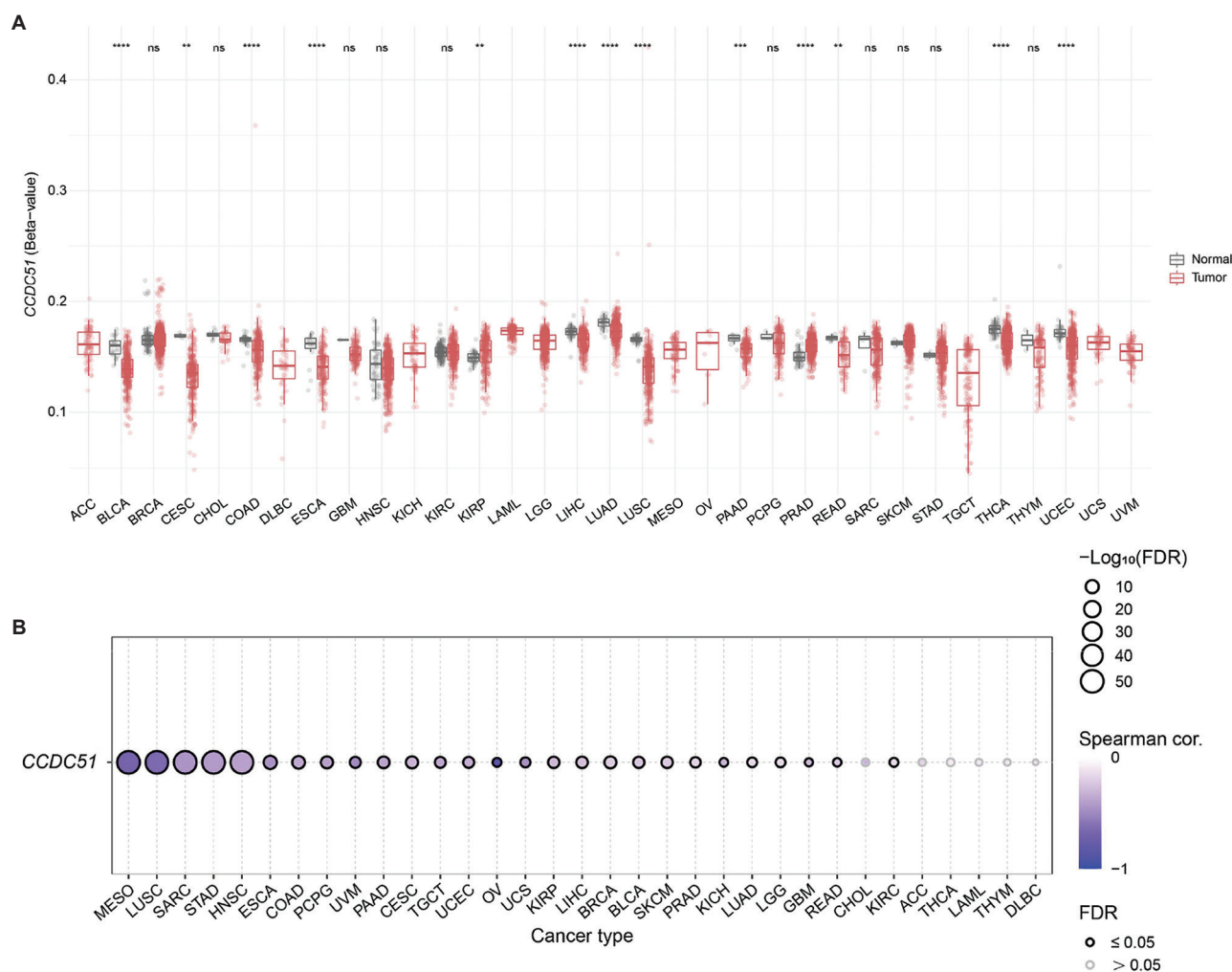


Figure 4. DNA methylation analysis of *CCDC51* across cancers. (A) DNA methylation levels of *CCDC51* across cancers. (B) Correlation between *CCDC51* expression and DNA methylation.

Notes: ** $p < 0.01$; **** $p < 0.0001$.

Abbreviations: FDR: False discovery rate; ns: Not significant.

cancer types, while negative correlations were observed in 13 others (Figure 5B). These results collectively suggest that *CCDC51* could significantly modulate antitumor immunity.

3.6. Immune infiltration of *CCDC51*

Analysis of the TIMER database indicated that *CCDC51* expression was significantly associated with 6 major immune cell types across 27 different cancer types (Figure 5C). Furthermore, *CCDC51* levels demonstrated strong correlations with the stromal score in 22 cancer types, the microenvironment score in 24 cancer types, and the immune score in both 19 and 38 cancer types (Figure 5D). These correlative findings suggest a potentially strong link between *CCDC51* expression and the extent of immune cell infiltration in diverse cancer contexts.

3.7. Prognostic analysis of *CCDC51* in HCC

Analysis of datasets from GSE14520, GSE54236, and GSE112790 (<https://www.ncbi.nlm.nih.gov/geo/>) revealed elevated *CCDC51* expression in HCC (Figure 6A). We next examined associations between *CCDC51* expression and HCC pathology, which demonstrated a significant correlation between high *CCDC51* levels and advanced histologic grade (Figure 6B). Furthermore, elevated *CCDC51* expression was associated with reduced OS across most clinical and demographic subgroups of HCC patients (Figure 6C). Multivariate Cox regression analysis further supported the prognostic value of *CCDC51* expression in HCC (Tables 1-3). In the TCGA-liver HCC cohort, both lower *CCDC51* expression and advanced pathological stage were identified as independent prognostic factors.

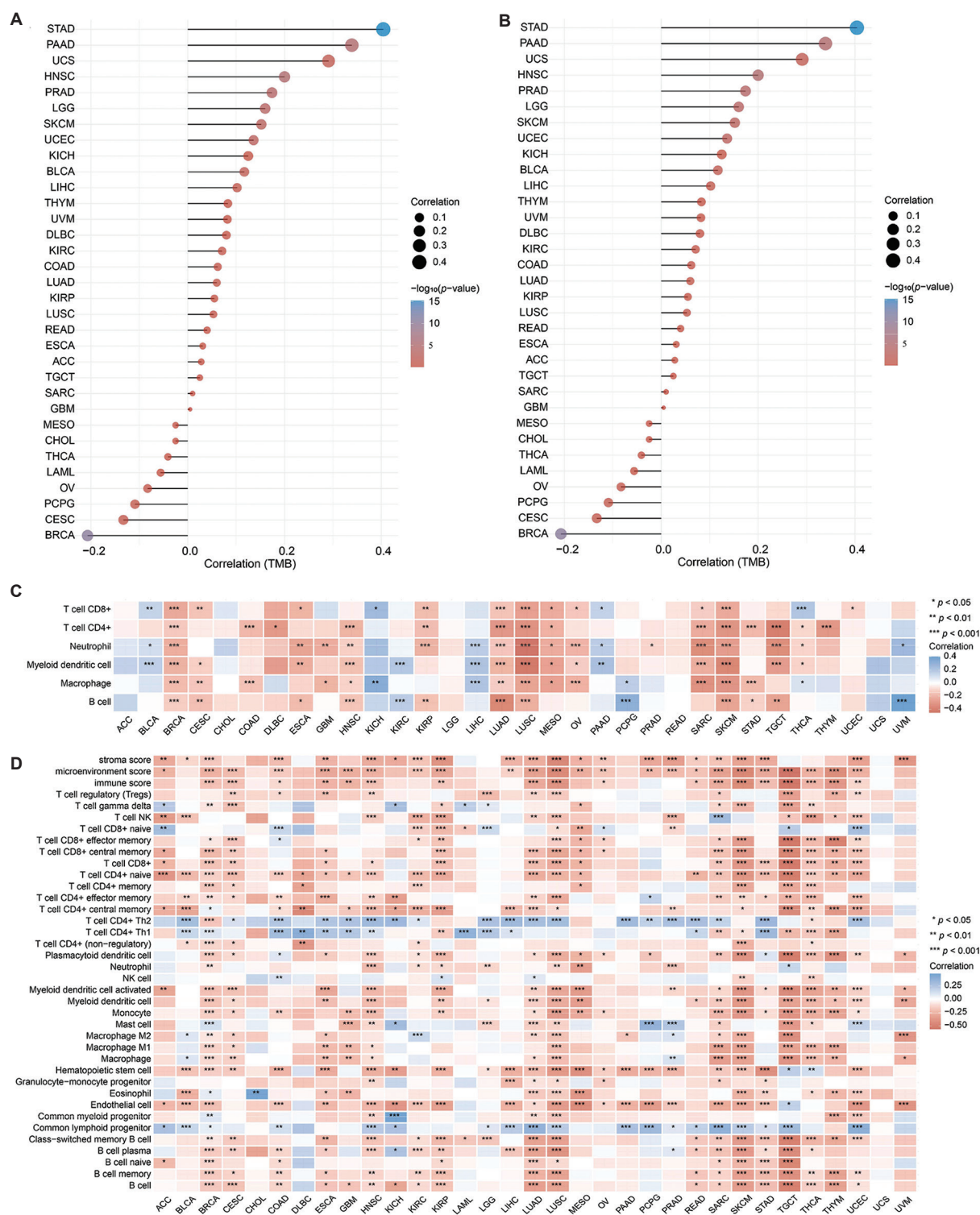


Figure 5. Relationships between *CCDC51* expression and TMB, MSI status, and immune infiltration. (A) Pan-cancer analysis of correlations between *CCDC51* expression levels and TMB. (B) Evaluation of the relationship linking *CCDC51* expression to MSI in diverse cancer types. (C) Correlation of *CCDC51* expression with immune cell infiltration levels in 33 human cancers, analyzed using the TIMER algorithm. (D) xCell-based assessment of connections between *CCDC51* expression and immune infiltration across 33 tumor types.

Notes: * $p < 0.05$, ** $p < 0.01$, *** $p < 0.001$.

Abbreviations: MSI: Microsatellite instability; TIMER: Tumor immune estimation resource; TMB: Tumor mutation burden.

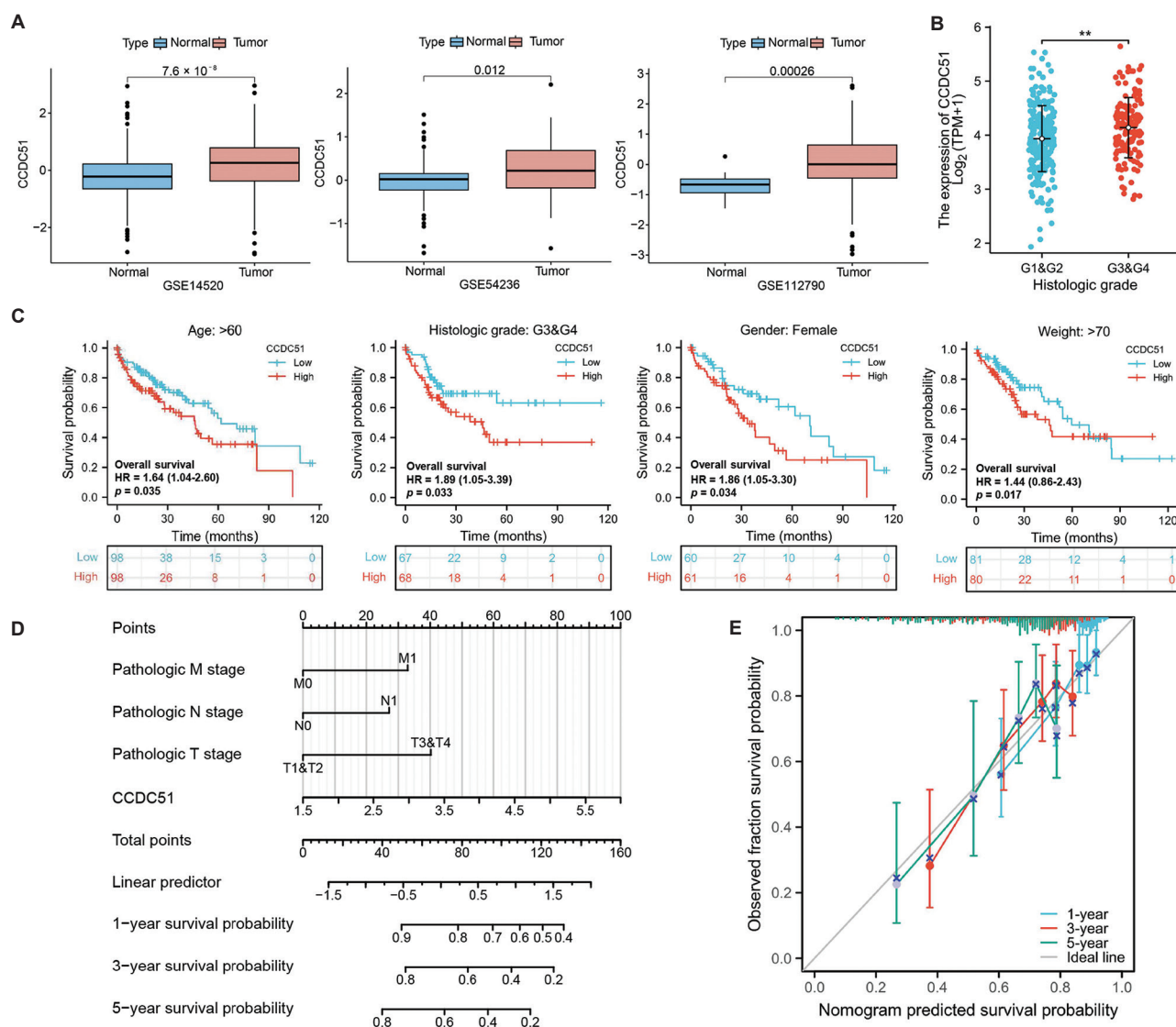


Figure 6. Prognostic analysis of *CCDC51* in HCC. (A) *CCDC51* expression levels in HCC analyzed using data from the GSE14520, GSE54236, and GSE112790 datasets. (B) Correlation between *CCDC51* expression and clinical characteristics in HCC. (C) Association of *CCDC51* expression with overall survival among different clinical subgroups of HCC patients. (D) A nomogram integrating TNM stage and *CCDC51* expression. (E) Predictive accuracy of the nomogram assessed via calibration curves at 1-, 3-, and 5-year intervals.

Note: ** $p < 0.01$.

Abbreviations: HCC: Hepatocellular carcinoma; TNM: Tumor, node, metastasis; TPM: Transcript per million.

To further assess the impact of *CCDC51* expression on HCC prognosis, univariate and multivariate Cox regression analyses of OS were performed, identifying N stage, M stage, T stage, and *CCDC51* expression as independent prognostic factors (Figure 6D). Calibration curves were subsequently employed to evaluate the predictive accuracy of the column-line diagram model at 1-, 3-, and 5-year intervals. These results demonstrated that *CCDC51* was crucial for OS prediction within the column-line diagram framework (Figure 6E). Thus, *CCDC51* may serve as a prognostic biomarker for survival in HCC patients.

3.8. Single-cell sequencing and spatial transcriptome analysis of *CCDC51* in HCC

To further characterize the *CCDC51* expression profile in HCC, we analyzed single-cell transcriptomic data. Analysis revealed predominant *CCDC51* expression in malignant cells (Figure 7A-C). Cell-cell communication analysis indicated enhanced interactions between *CCDC51*⁺ malignant cells and macrophages (Figure 7D). Furthermore, pathway analysis revealed elevated activity in metabolic and proliferative processes within *CCDC51*⁺

Table 1. Univariate and multivariate Cox regression analyses of the effects of different parameters on overall survival in hepatocellular carcinoma patients

Characteristics	Total (n)	Univariate analysis		Multivariate analysis	
		Hazard ratio (95% CI)	p-value	Hazard ratio (95% CI)	p-value
T stage	370				
T1 and T2	277	Reference			
T3 and T4	93	2.598 (1.826–3.697)	< 0.001	1.906 (0.255–14.267)	0.530
N stage	258				
N0	254	Reference			
N1	4	2.029 (0.497–8.281)	0.324		
M stage	272				
M0	268	Reference			
M1	4	4.077 (1.281–12.973)	0.017	1.500 (0.354–6.349)	0.582
Pathologic stage	349				
Stage I and II	259	Reference			
Stage III and IV	90	2.504 (1.727–3.631)	< 0.001	1.270 (0.170–9.483)	0.816
Tumor status	354				
Tumor free	202	Reference			
With tumor	152	2.317 (1.590–3.376)	< 0.001	1.959 (1.228–3.124)	0.005
CCDC51 expression	373	1.826 (1.265–2.636)	0.001	1.858 (1.148–3.006)	0.012

Abbreviation: CI: Confidence interval.

Table 2. Univariate and multivariate Cox regression analyses of the effects of different parameters on disease-specific survival in hepatocellular carcinoma patients

Characteristics	Total (n)	Univariate analysis		Multivariate analysis	
		Hazard ratio (95% CI)	p-value	Hazard ratio (95% CI)	p-value
T stage	362				
T1 and T2	272	Reference			
T3 and T4	90	3.639 (2.328–5.688)	< 0.001	14.664 (0.831–258.901)	0.067
N stage	253				
N0	249	Reference			
N1	4	3.612 (0.870–14.991)	0.077	9.936 (1.242–79.495)	0.030
M stage	268				
M0	265	Reference			
M1	3	5.166 (1.246–21.430)	0.024	2.319 (0.533–10.081)	0.262
Pathologic stage	341				
Stage I and II	254	Reference			
Stage III and IV	87	3.803 (2.342–6.176)	< 0.001	0.279 (0.015–5.202)	0.392
Tumor status	354				
Tumor free	202	Reference			
With tumor	152	NA	NA		
CCDC51 expression	365	1.768 (1.101–2.840)	0.018	1.842 (0.893–3.797)	0.098

Note: Analysis for the “with tumor” group is unavailable as there are zero events in the reference group.

Abbreviations: CI: Confidence interval; NA: Not applicable.

Table 3. Univariate and multivariate Cox regression analyses of the influence of different parameters on the progression-free interval in hepatocellular carcinoma patients

Characteristics	Total (n)	Univariate analysis		Multivariate analysis	
		Hazard ratio (95% CI)	p-value	Hazard ratio (95% CI)	p-value
T stage	370				
T1 and T2	277	Reference			
T3 and T4	93	2.177 (1.590–2.980)	<0.001	0.864 (0.207–3.605)	0.841
N stage	258				
N0	254	Reference			
N1	4	1.370 (0.338–5.552)	0.659		
M stage	272				
M0	268	Reference			
M1	4	3.476 (1.091–11.076)	0.035	1.471 (0.451–4.804)	0.522
Pathologic stage	349				
Stage I and II	259	Reference			
Stage III and IV	90	2.201 (1.591–3.046)	<0.001	2.044 (0.489–8.548)	0.327
Tumor status	354				
Tumor free	202	Reference			
With tumor	152	11.342 (7.567–17.000)	< 0.001	15.329 (9.216–25.497)	<0.001
CCDC51 expression	373	1.234 (0.904–1.686)	0.186		

Abbreviation: CI: Confidence interval.

malignant cells (Figure 7E). Spatial transcriptomic profiling of HCC tissues revealed enriched *CCDC51* expression in malignant tumor regions (Figure 7F-I).

3.9. Biological function analysis of *CCDC51* in HCC

For kyoto encyclopedia of genes and genomes and gene ontology enrichment analyses of *CCDC51* in HCC, the GEPIA database was employed to determine the 50 most correlated genes (Figure 8A). Enrichment analysis revealed that these genes were primarily enriched in biological processes closely related to liver cancer, such as mitochondrial function and pseudouridine synthase activity (Figure 8B and C). These findings indicate that *CCDC51* may play a key role in regulating the malignant progression of HCC.

3.10. Knockdown of *CCDC51* suppresses the malignant phenotype of HCC

Analysis of TCGA–liver HCC data revealed significantly elevated *CCDC51* expression in HCC compared to matched adjacent non-tumor tissues (Figure 9A). Immunohistochemical staining using the HPA database showed substantially higher *CCDC51* protein levels in tumors than in normal tissues (Figure 9B). To functionally characterize *CCDC51* in HCC, we performed *in vitro* experiments. The efficacy of siRNA-mediated *CCDC51* knockdown was confirmed by Western blot analysis

in HCCLM3 and Hep3B cells (Figure 9C, Figure A1). *CCDC51* silencing significantly impaired proliferation, migration, and invasion in both HCCLM3 and Hep3B cell lines (Figure 9D-F). These findings indicate a tumor-promoting role for *CCDC51* in HCC.

4. Discussion

HCC remains a leading cause of cancer-related mortality worldwide, posing a significant and persistent threat to global public health. Its high incidence, particularly in regions endemic for hepatitis B and C viral infections, coupled with frequent late-stage diagnosis and limited therapeutic options for advanced disease, contributes substantially to its poor prognosis and heavy societal burden.^{22–24} Over the past decades, substantial research efforts have been dedicated to unraveling the complex molecular pathogenesis of HCC, aiming to identify reliable prognostic biomarkers and novel therapeutic targets.^{25,26} Alterations in key signaling pathways governing cell proliferation, apoptosis, and metastasis are central to hepatocarcinogenesis. Despite advancements, the clinical translation of numerous molecular discoveries remains challenging, underscoring the urgent need to identify and validate new drivers of HCC progression. In this context, the role of specific genes encoding structural or regulatory proteins in the tumor microenvironment and their impact on patient outcomes are areas of intense investigation.

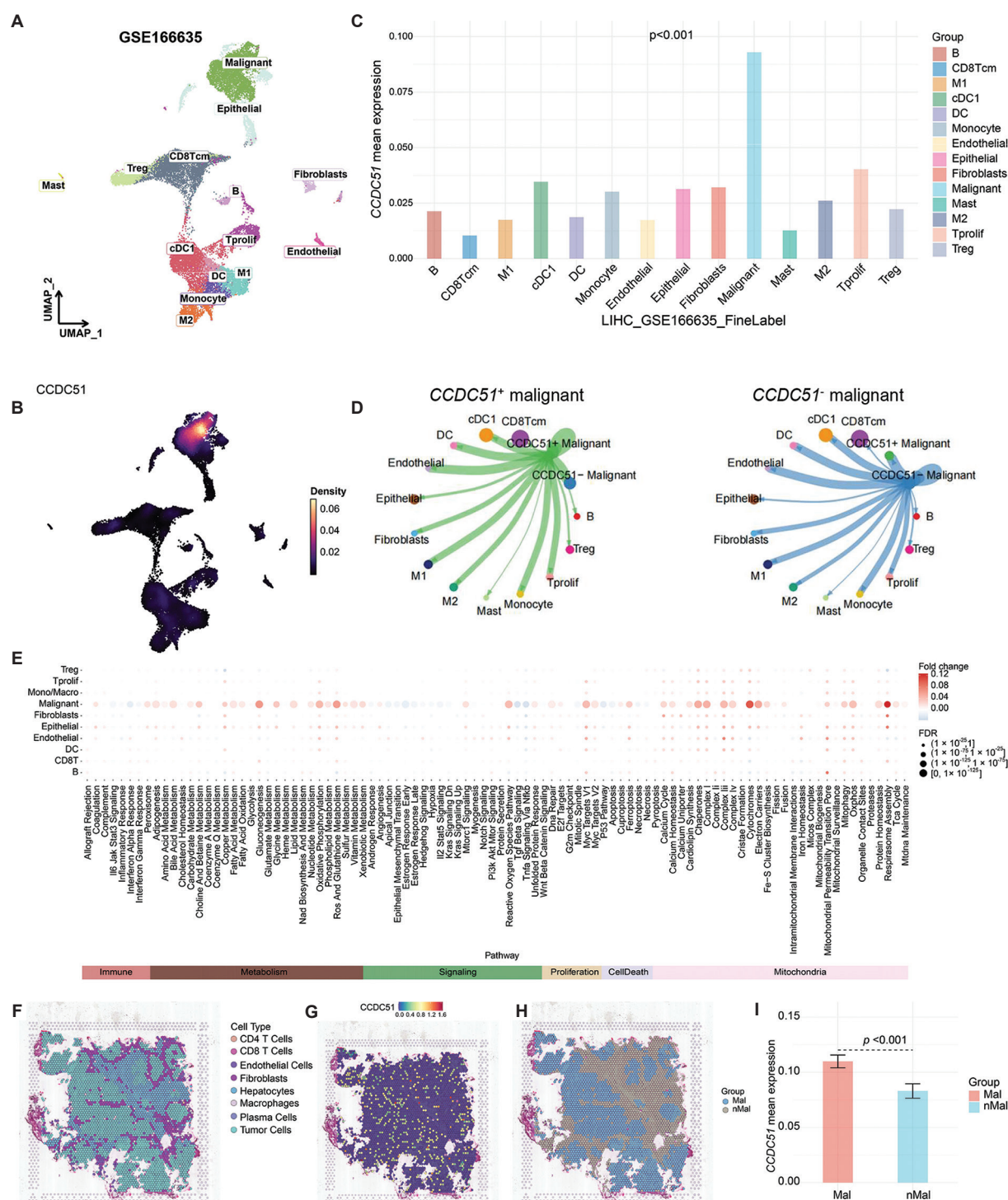
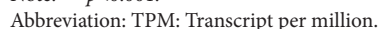


Figure 7. Single-cell sequencing and spatial transcriptome analysis of *CCDC51* in HCC. (A) UMAP visualization depicting the cellular architecture within the GSE166635 single-cell dataset. (B) FeaturePlot visualization of *CCDC51* expression patterns across heterogeneous cell populations, enabling comparative analysis of transcript abundance. (C) Mean *CCDC51* transcript levels across distinct cell populations. (D) Network analysis revealing interaction patterns between *CCDC51*⁺ and *CCDC51*⁻ malignant cells. (E) Pathway activity disparities between cell subtypes stratified by *CCDC51* expression status. (F) Spatial distribution of unannotated cells within HCC tissue sections. (G) Spatial mapping of *CCDC51* expression throughout HCC tissue. (H) Segmentation of tumor and adjacent non-tumor regions in HCC spatial transcriptomes. (I) Bar graph quantifying mean *CCDC51* expression levels across experimental groups.

Abbreviations: FDR: False discovery rate; HCC: Hepatocellular carcinoma; UMAP: Uniform Manifold Approximation and Projection.



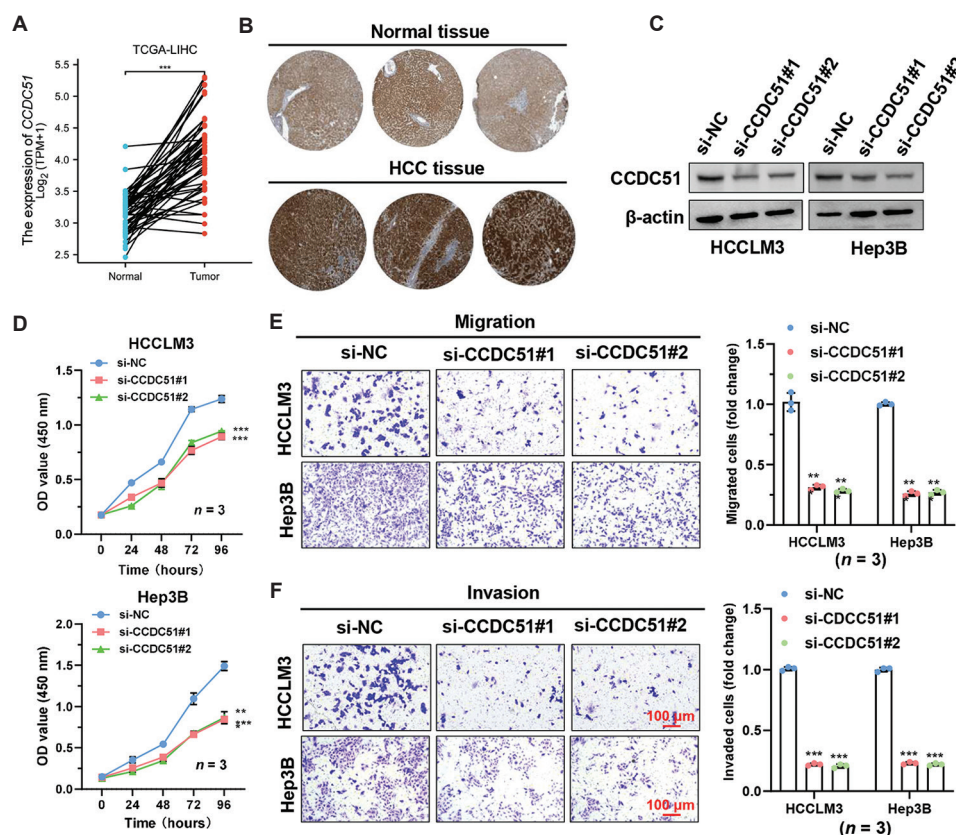


Figure 9. *CCDC51* promotes the proliferation, migration, and invasion of HCC cells. (A) Analysis of *CCDC51* expression levels in HCC tissues versus adjacent normal tissues. (B) Representative immunohistochemistry images illustrating *CCDC51* protein expression in normal liver tissues and HCC tissues from the Human Protein Atlas.²¹ Scale bar: 100 μ m. (C) Western blot analysis confirming *CCDC51*-knockdown in HCCLM3 and Hep3B cell lines. (D) Silencing of *CCDC51* significantly inhibited the proliferation of HCCLM3 and Hep3B cells, as determined by Cell Counting Kit-8 assays. (E, F) *CCDC51* knockdown markedly suppressed migration and invasion capacities in both HCCLM3 and Hep3B cell lines. Scale bar: 100 μ m. All data are presented as mean \pm standard deviation from three independent experiments.

Notes: ** $p < 0.01$; *** $p < 0.001$.

Abbreviations: *CCDC51*: Coiled-coil domain-containing 51 protein; HCC: Hepatocellular carcinoma; LIHC: Liver hepatocellular carcinoma; NC: Negative control; OD: Optical density; TCGA: The Cancer Genome Atlas; TPM: Transcript per million.

Our study focuses on elucidating the function and clinical significance of *CCDC51* in HCC.

We systematically investigated *CCDC51* expression patterns across multiple human cancers. Our analysis identified substantial upregulation of *CCDC51* in 24 malignant tissue types compared to corresponding normal tissues. Elevated *CCDC51* expression was further correlated with unfavorable clinical outcomes, including reduced OS in diverse cancers. ROC curve analyses validated the diagnostic potential of *CCDC51*, showing high sensitivity and specificity across several malignancies. Notably, patients with mature B-cell neoplasms had the highest frequency of *CCDC51* genetic alterations, exceeding 6% (based on the knowledge library information regarding mature B-cell neoplasms).¹⁴

TMB and MSI are established biomarkers predictive of response to ICB in cancer.^{18,19} Our correlative analyses

suggested that *CCDC51* expression was associated with stromal score, immune microenvironment score, and immune score across multiple cancer types. These associations may indicate a potential link between *CCDC51* levels and immune cell infiltration within the tumor microenvironment. The association between *CCDC51* expression and immune infiltration suggests its possible role in modulating the tumor immune microenvironment, which plays a crucial role in tumor progression and immune escape.

Analysis of the TCGA-liver HCC cohort identified *CCDC51* expression levels and pathological stage as independent prognostic factors. To further investigate the functional relevance of *CCDC51* in HCC, enrichment analyses were performed, indicating its involvement in HCC-associated signaling pathways and biological processes. In addition, *CCDC51* was found to be significantly overexpressed in HCC cell lines. Examination

of single-cell and spatial transcriptomic data from liver cancer specimens revealed elevated *CCDC51* expression in malignant cells, suggesting its potential functional role in HCC. Finally, *CCDC51* silencing was associated with reduced proliferative, migratory, and invasive capacities in these cancer cells.

In summary, these findings suggest the diverse functional contributions of *CCDC51* in HCC, supporting its potential utility as both a biomarker and therapeutic target for clinical translation. Nevertheless, several fundamental questions persist without definitive answers and merit deeper inquiry. Our initial pan-cancer analysis primarily identified correlative associations between *CCDC51* and immune cell infiltration, which, while suggestive, require experimental validation to clarify its possible function in TMB-associated immune regulation during oncogenesis. Moreover, rigorous *in vivo* studies are required to further evaluate the role of *CCDC51* in HCC pathogenesis, as elucidating this mechanism may offer pivotal insights into the development of innovative treatment modalities.

5. Conclusion

Our results indicate that *CCDC51* is crucial for HCC progression and may serve as a valuable target for diagnostic and therapeutic approaches.

Acknowledgments

We are grateful for the support of Home for Research (www.home-for-researchers.com).

Funding

This study was supported by the Wenzhou Science and Technology Bureau Research Project of China (Y2023912).

Conflict of interest

The authors declare they have no competing interests.

Author contributions

Conceptualization: Xiaoyan Huang

Formal analysis: Siqi Huang, Wei Yu

Investigation: Siqi Huang, Zhang Chen

Methodology: Siqi Huang, Xiaoyan Huang

Writing – original draft: Siqi Huang, Zhang Chen, Wei Yu

Writing – review & editing: Siqi Huang, Xiaoyan Huang

Ethics approval and consent to participate

Not applicable.

Consent for publication

Not applicable.

Availability of data

Data available on request from the authors.

Further disclosure

The results sections corresponding to [Figure 1–5](#), [Figure 8](#), and [Table 1–3](#) in the main text have been uploaded to or deposited in a preprint server (DOI: 10.22541/au.168547510.04853738/v1).

References

- Bray F, Laversanne M, Sung H, *et al.* Global cancer statistics 2022: GLOBOCAN estimates of incidence and mortality worldwide for 36 cancers in 185 countries. *CA Cancer J Clin.* 2024;74(3):229–263.
doi: 10.3322/caac.21834
- Xia C, Dong X, Li H, *et al.* Cancer statistics in China and United States, 2022: Profiles, trends, and determinants. *Chin Med J (Engl).* 2022;135(5):584–590.
doi: 10.1097/cm9.0000000000002108
- Nagaraju GP, Dariya B, Kasa P, Peela S, El-Rayes BF. Epigenetics in hepatocellular carcinoma. *Semin Cancer Biol.* 2022;86(Pt 3):622–632.
doi: 10.1016/j.semcancer.2021.07.017
- Wang Q, Yu P, Liu C, He X, Wang G. Mitochondrial fragmentation in liver cancer: Emerging player and promising therapeutic opportunities. *Cancer Lett.* 2022;549:215912.
doi: 10.1016/j.canlet.2022.215912
- Dai F, Yuan Y, Hao J, *et al.* PDCD₂ as a prognostic biomarker in glioma correlates with malignant phenotype. *Genes Dis.* 2024;11(5):101106.
doi: 10.1016/j.gendis.2023.101106
- Guo Q, Zhao L, Yan N, *et al.* Integrated pan-cancer analysis and experimental verification of the roles of tropomyosin 4 in gastric cancer. *Front Immunol.* 2023;14:1148056.
doi: 10.3389/fimmu.2023.1148056
- Zeitz C, Méjécase C, Michiels C, *et al.* Mutated *CCDC51* coding for a mitochondrial protein, MITOK is a candidate gene defect for autosomal recessive rod-cone dystrophy. *Int J Mol Sci.* 2021;22(15):7875.
doi: 10.3390/ijms22157875
- Tang Z, Li C, Kang B, Gao G, Li C, Zhang Z. GEPIA: A web server for cancer and normal gene expression profiling and interactive analyses. *Nucleic Acids Res.* 2017;45(W1):W98–W102.
doi: 10.1093/nar/gkx247
- Mizuno H, Kitada K, Nakai K, Sarai A. PrognoScan: A new database for meta-analysis of the prognostic value of genes.

- BMC Med Genomics*. 2009;2:18.
doi: 10.1186/1755-8794-2-18
10. Shi J, Wei X, Xun Z, *et al*. The web-based portal SpatialTME integrates histological images with single-cell and spatial transcriptomics to explore the tumor microenvironment. *Cancer Res*. 2024;84(8):1210-1220.
doi: 10.1158/0008-5472.can-23-2650
 11. Xun Z, Ding X, Zhang Y, *et al*. Reconstruction of the tumor spatial microenvironment along the malignant-boundary-nonmalignant axis. *Nat Commun*. 2023;14(1):933.
doi: 10.1038/s41467-023-36560-7
 12. Thorsson V, Gibbs DL, Brown SD, *et al*. The immune landscape of cancer. *Immunity*. 2019;51(2):411-412.
doi: 10.1016/j.immuni.2019.08.004
 13. Bonneville R, Krook MA, Kautto EA, *et al*. Landscape of microsatellite instability across 39 cancer types. *JCO Precis Oncol*. 2017;1:1-15.
doi: 10.1200/po.17.00073
 14. Cerami E, Gao J, Dogrusoz U, *et al*. The cBio cancer genomics portal: An open platform for exploring multidimensional cancer genomics data. *Cancer Discov*. 2012;2(5):401-404.
doi: 10.1158/2159-8290.cd-12-0095
 15. Xiang J, Guo S, Jiang S, *et al*. Silencing of long non-coding RNA MALAT1 promotes apoptosis of glioma cells. *J Korean Med Sci*. 2016;31(5):688-694.
doi: 10.3346/jkms.2016.31.5.688
 16. Datta I, Noushmehr H, Brodie C, *et al*. Expression and regulatory roles of lncRNAs in G-CIMP-low vs G-CIMP-high Glioma: An *in-silico* analysis. *J Transl Med*. 2021;19(1):182.
doi: 10.1186/s12967-021-02844-z
 17. Wang J, Zhang M, Lu W. Long noncoding RNA GACAT3 promotes glioma progression by sponging miR-135a. *J Cell Physiol*. 2019;234(7):10877-10887.
doi: 10.1002/jcp.27946
 18. Li X, Luo Y, Liu L, *et al*. The long noncoding RNA ZFAS1 promotes the progression of glioma by regulating the miR-150-5p/PLP2 axis. *J Cell Physiol*. 2020;235(3):2937-2946.
doi: 10.1002/jcp.29199
 19. Tang C, Wang Y, Zhang L, *et al*. Identification of novel lncRNA targeting Smad2/PKC α signal pathway to negatively regulate malignant progression of glioblastoma. *J Cell Physiol*. 2020;235(4):3835-3848.
doi: 10.1002/jcp.29278
 20. Xu H, Zhao G, Zhang Y, *et al*. Long non-coding RNA PAXIP1-AS1 facilitates cell invasion and angiogenesis of glioma by recruiting transcription factor ETS1 to upregulate KIF14 expression. *J Exp Clin Cancer Res*. 2019;38(1):486.
doi: 10.1186/s13046-019-1474-7
 21. Colwill K, Renewable Protein Binder Working Group, Susanne Gräslund. A roadmap to generate renewable protein binders to the human proteome. *Nat Methods*. 2011;8(7):551-558.
doi: 10.1038/nmeth.1607
 22. Ganne-Carrié N, Nahon P. Differences between hepatocellular carcinoma caused by alcohol and other aetiologies. *J Hepatol*. 2025;82(5):909-917.
doi: 10.1016/j.jhep.2024.12.030
 23. Alawiyia B, Constantinou C. Hepatocellular carcinoma: A narrative review on current knowledge and future prospects. *Curr Treat Options Oncol*. 2023;24(7):711-724.
doi: 10.1007/s11864-023-01098-9
 24. Yang T, Wang MD, Xu XF, Li C, Wu H, Shen F. Management of hepatocellular carcinoma in China: Seeking common grounds while reserving differences. *Clin Mol Hepatol*. 2023;29(2):342-344.
doi: 10.3350/cmh.2023.0106
 25. Xue Y, Ruan Y, Wang Y, Xiao P, Xu J. Signaling pathways in liver cancer: Pathogenesis and targeted therapy. *Mol Biomed*. 2024;5(1):20.
doi: 10.1186/s43556-024-00184-0
 26. Cao LQ, Xie Y, Fleishman JS, Liu X, Chen ZS. Hepatocellular carcinoma and lipid metabolism: Novel targets and therapeutic strategies. *Cancer Lett*. 2024;597:217061.
doi: 10.1016/j.canlet.2024.217061

Appendix

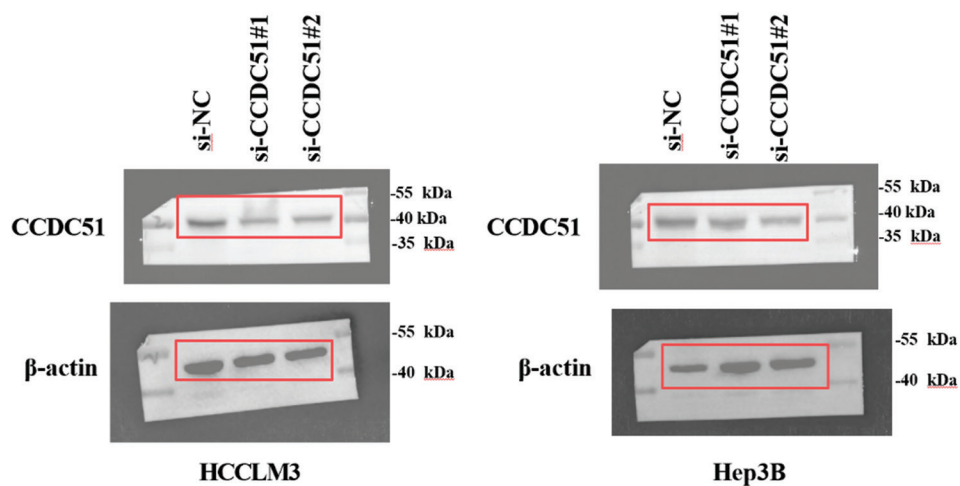


Figure A1. Original images for Western blot results for CCDC51 and β-actin in [Figure 9C](#)
Abbreviation: CCDC51: Coiled-coil domain-containing protein 51.